Subgrid scale modeling in solar convection simulations using the ASH code

By Y.-N. Young, M. Miesch† and N. N. Mansour

1. Motivation and objectives

The turbulent solar convection zone has remained one of the most challenging and important subjects in physics. Understanding the complex dynamics in the solar convection zone is crucial for gaining insight into the solar dynamo problem. Many solar observatories have generated revealing data with great details of large scale motions in the solar convection zone. For example, a strong differential rotation is observed: the angular rotation is observed to be faster at the equator than near the poles not only near the solar surface, but also deep in the convection zone. On the other hand, due to the wide range of dynamical scales of turbulence in the solar convection zone, both theory and simulation have limited success. Thus, cutting edge solar models and numerical simulations of the solar convection zone have focused more narrowly on a few key features of the solar convection zone, such as the time-averaged differential rotation. For example, Brun & Toomre (2002) report computational finding of differential rotation in an anelastic model for solar convection. A critical shortcoming in this model is that the viscous dissipation is based on application of mixing length theory to stellar dynamics with some *ad hoc* parameter tuning.

The goal of our work is to implement the subgrid scale model developed at CTR into the solar simulation code and examine how the differential rotation will be affected as a result. Specifically, we implement a Smagorinsky-Lilly subgrid scale model into the ASH (anelastic spherical harmonic) code developed over the years by various authors. Readers are referred to (Clune *et al.* 1999) and (Miesch 1998) for a detailed description of the ASH code. This paper is organized as follows. In §2 we briefly formulate the anelastic system that describes the solar convection. In §3 we formulate the Smagorinsky-Lilly subgrid scale model for unstably stratified convection. We then present some preliminary results in §4, where we also provide some conclusions and future directions.

2. The anelastic equations of motions

In the solar convection zone, the depth extends over many density scale heights and thus the effects of stratification need to be captured despite the fact that acoustic timescales are much shorter than the large-scale convection timescales. An appropriate approach is to filter out sound waves while maintaining the density stratification, namely the anelastic approximation first proposed by Gough (1969) and later adapted to the solar convection zone by Gilman & Glatzmaier (1981). In stellar models, a fluid layer is unstable if the layer is superadiabatic. The degree of superadibaticity is quantified as

† High Altitude Observatory, National Center for Atmospheric Research, Boulder, Colorado, 80301

(Gilman & Glatzmaier 1981)

$$\epsilon \equiv -\frac{d}{C_P}\left(\frac{\partial s}{\partial r}\right)_0, \tag{2.1}$$

where d is the depth of the convection zone, C_P the specific heat capacity at constant pressure, s the entropy, and r the radial coordinate. The entropy gradient is calculated at some fiducial level in the convection zone. In the sun, the departure from adiabaticity in the convection zone is extremely small (Christensen-Dalsgaard *et al.* 1993),

$$\epsilon \leq 10^{-4}. \tag{2.2}$$

If we assume that the velocity in the horizontal (transverse to gravity) directions is mostly driven by pressure gradients, the coupling between vertical and horizontal velocities leads to the following relationship between the convection velocity v and sound speed c_s

$$\mathcal{M} \equiv \frac{v}{c_s} \sim \sqrt{\epsilon} \ll 1, \tag{2.3}$$

where $\mathcal{M}$ is the Mach number of the flow.

The basic idea in the anelastic approximation is to expand the variables in terms of the small parameter ϵ, and collect terms of the zeroth and first orders. As is usually found in perturbation theory, the zeroth order equations describe the basic state, which remain stationary over timescales at which the first order variables vary. The fundamental equations are the compressible, stratified Navier-Stokes equations in a rotating reference frame

$$\rho\left(\frac{\partial \mathbf{v}}{\partial t} + (\mathbf{v}\cdot\nabla)\mathbf{v}\right) = -\nabla P + \rho\mathbf{g} + 2\mathbf{v}\times\Omega_0 + \nabla\cdot\mathcal{D}, \tag{2.4}$$

$$\rho\Theta\frac{\partial s}{\partial t} + \rho\Theta\mathbf{v}\cdot\nabla s = -\nabla\cdot q + 2\nu\rho\left(e_{ij}e_{ij} - \frac{1}{3}(\nabla\cdot\mathbf{v})^2\right) - \rho\mathcal{E}, \tag{2.5}$$

$$\frac{\partial \rho}{\partial t} + \nabla\cdot(\rho\mathbf{v}) = 0, \tag{2.6}$$

where s is the entropy, Θ is the temperature, and $\mathcal{E}$ is the nuclear energy generation rate. The viscous stress $\mathcal{D}$ is defined as

$$\mathcal{D} \equiv 2\rho\nu\left(e_{ij} - \frac{1}{3}(\nabla\cdot\mathbf{v})\delta_{ij}\right), \tag{2.7}$$

and q is the composite non-convective heat flux, defined as

$$q \equiv -\kappa\rho\Theta\nabla s - \kappa_r\rho C_p\nabla\Theta. \tag{2.8}$$

and the various transport coefficient such as the viscosity ν, thermal diffusion κ, and radiative thermal diffusion κ_r are assumed to be functions of the radial coordinate only.

Upon substituting the variables expanded in terms of the small parameter ϵ, at zeroth order we obtain the hydrostatic equation. Denoting the zeroth order terms with a subscript 0, the equations at the leading order are

$$\frac{\partial P_0}{\partial r} + \Lambda = -\rho_0 g, \tag{2.9}$$

$$P_0 = \mathcal{R}\rho_0\Theta_0, \tag{2.10}$$

where Λ is the radial gradient of a mean turbulent pressure

$$\Lambda \equiv \langle [\rho_0(\mathbf{v}\cdot\nabla)\mathbf{v} - \nabla\cdot\mathcal{D} - 2\rho_0(\mathbf{v}\times\Omega_0)]_r\rangle_t\,. \tag{2.11}$$

The angular brackets in Equation (2.11) denote horizontal averages, and the square brackets denote the radial component of the enclosed vector. We evaluate Λ only as we update the reference state (denoted with a subscript 0).

At the next order, we obtain the anelastic equations for compressible, stratified fluids

$$\frac{\partial \rho_0\mathbf{v}}{\partial t} + \rho_0(\mathbf{v}\cdot\nabla)\mathbf{v} = -\nabla P + \nabla\cdot\mathcal{D} + \rho\mathbf{g} + 2\rho_0(\mathbf{v}\times\Omega_0) + \Lambda\hat{r}, \tag{2.12}$$

$$\begin{aligned}\rho_0\Theta_0\frac{\partial s}{\partial t} + \rho_0\Theta_0\mathbf{v}\cdot\nabla(s_0+s) = \nabla\cdot(\kappa\rho_0\Theta_0\nabla(s_0+s) + \kappa_r\rho_0 C_p\nabla(\Theta_0+\Theta))\\ +2\nu\rho_0\left(e_{ij}e_{ij} - \frac{1}{3}(\nabla\cdot\mathbf{v})^2\right) - \rho_0\mathcal{E},\end{aligned} \tag{2.13}$$

$$\nabla\cdot(\rho_0\mathbf{v}) = 0, \tag{2.14}$$

and

$$\frac{\rho}{\rho_0} = \frac{P}{P_0} - \frac{\Theta}{\Theta_0} = \frac{P}{\gamma P_0} - \frac{s}{C_p}. \tag{2.15}$$

We note that both the reference state and perturbation terms have been retained in Equation (2.13) because the gradient of the reference state entropy (s_0) varies in amplitude from $\mathcal{O}(\epsilon)$ in the convection zone to $\mathcal{O}(1)$ in the convectively stable region. This scaling is also true for the term involving thermal diffusion of the reference temperature ($\kappa_r\partial\Theta_0/\partial r$). We retain the term $\kappa_r\partial\Theta/\partial r$ because we wish to allow for small deviations of the radiative heat flux from spherical symmetry.

The viscosity coefficient ν is assumed to be a function of the reference density ρ_0. The functional dependence is obtained from mixing length theory, and the specific value is chosen in an *ad hoc* fashion for a given numerical resolution and combination of parameters. Our main goal in this work is to replace these "mixing length" viscosity and thermal diffusivity with those based on Smagorinsky subgrid scale model. More details will be presented in §3.

The reference state is crucial in the simulation of the anelastic system. In the ASH code, the reference state is updated only every few hundred steps of advancing the anelastic equations. During the update process, the following equations are solved simultaneously for the reference pressure P_0 and density ρ_0:

$$\frac{1}{C_P}\frac{ds_0}{dr} = \frac{1}{\gamma}\frac{d\ln P_0}{dr} - \frac{d\ln\rho_0}{dr}, \tag{2.16}$$

$$\frac{dP_0}{dr} = -\rho_0 g. \tag{2.17}$$

Using the reference entropy gradient (ds_0/dr) and gravity ($g(r)$) profiles from the previous time step, Equations (2.16) and (2.17) are solved for the reference pressure and density. Figure 1 is an example from one of the ASH simulations. With similar reference states and viscosity profiles to those illustrated in figure 1, simulations of the ASH code have successfully generated differential rotation profiles that are similar to the solar observations. An example from ASH simulations is illustrated in figure 2. The numerical resolution for figure 2 is $65\times128\times256$ in the radial, latitudinal, and azimuthal

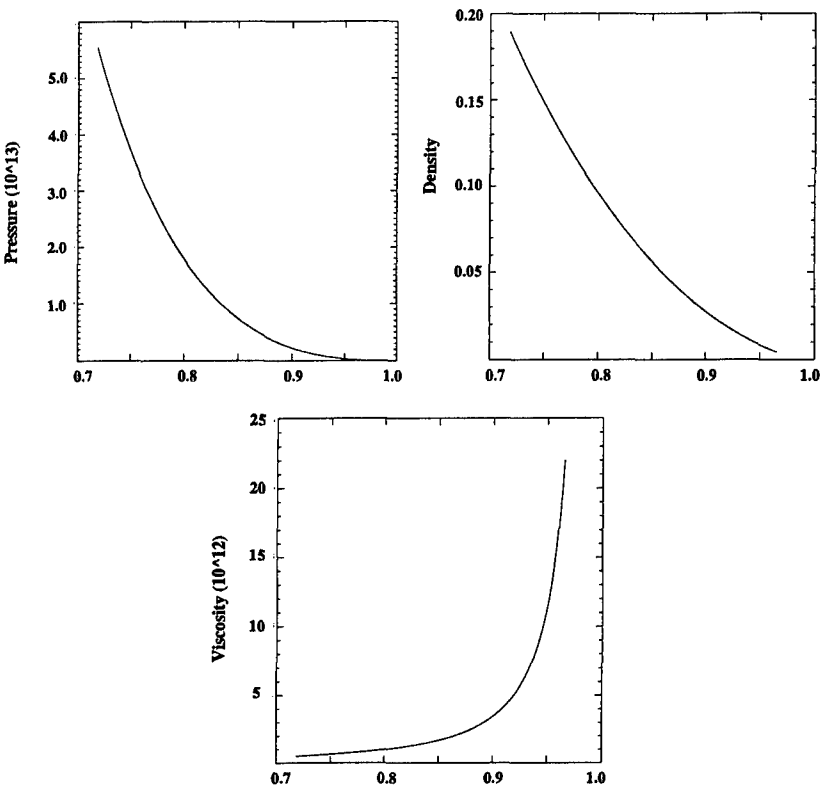

FIGURE 1. Reference state from ASH simulations, the horizontal axis is radial coordinate in units of solar radius. Panel (a): Reference pressure (dyne/cm^2) within the convection zone. Panel (b): Reference density (g/cm^3). Panel (c): the "mixing length" viscosity (cm^2/sec) as a function of r.

directions. The left panel is a filled contour plot of the averaged angular velocity as a function of latitude and radius, while the right panel shows the angular velocity at five latitudes as a function of radius from the bottom to the top of the convection zone. For this particular case, the viscosity is a prescribed function of radius as shown in figure 1(c), and the Prandtl number is fixed at 1/4. This corresponds to the AB case in Brun & Toomre (2002), in which the differential rotation inside the convection zone is most prominent among all the simulation data presented in Brun & Toomre (2002). Figure 2 is from simulations conducted on the NASA/Ames SGI cluster with different initial conditions. A typical differential rotation from solar helioseismic observations is shown in figure 2(c) (same as figure 1(b) in Brun & Toomre (2002)). The close similarity between observational solar differential rotation and the simulation data shows great promise that better results may be obtainable if the conveciton model is refined by building in more physics. For example, the viscosity and thermal diffusivity may be replaced by better dynamical models. Addition of a mechanism to couple the convection zone with the tachocline below may result in better agreement between simulation and observational data. As a preliminary initiative we have undertaken is to first improve the model for viscosity using Smagorinsky-Lilly's model.

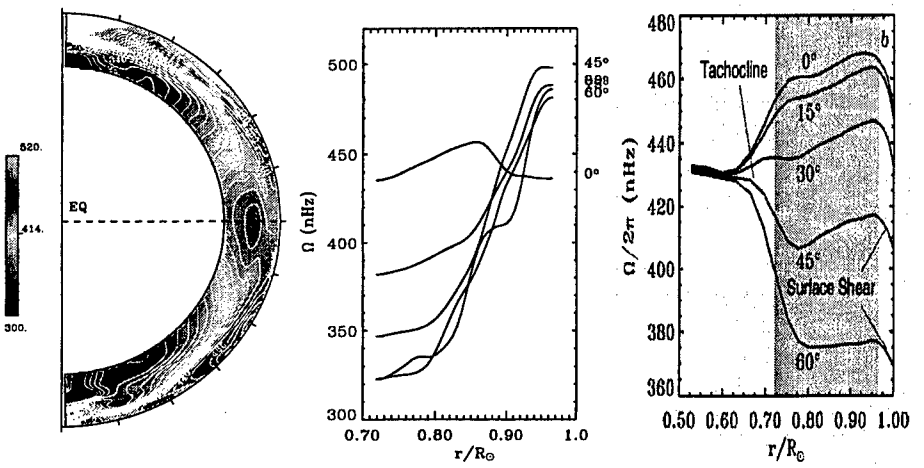

FIGURE 2. Panels (a) and (b): Differential rotation for the AB case in Brun & Toomre (2002) with different initial conditions. Panel (c) is the time-averaged rotation rates from five years of GONG data.

3. Smagorinsky-Lilly subgrid scale model

The principle underlying the Smagorinsky subgrid scale model is the balance of production of subgrid-scale turbulent kinetic energy and dissipation of isotropic turbulence energy at the characteristic eddy size. Let the subgrid turbulent production rate be denoted by $\mathcal{P}$, then for a given turbulent viscosity ν_T, the subgrid turbulent production rate is

$$\mathcal{P} = 2\nu_T e_{ij} e_{ij}. \tag{3.1}$$

The dissipation at scale l is $\sim q^3/l$, where q is a characteristic turbulent velocity. Finally, to find an expression for ν_T in terms of the resolved quantities, we utilize the Prandtl's assumption: $\nu_T = C_1 q l$, and upon substituting q into the dissipation rate and equating dissipation and production rates, we obtain the Smagorinsky subgrid scale model

$$\nu_T = (C_s l)^2 \sqrt{2 e_{ij} e_{ij}}, \tag{3.2}$$

where C_s is a constant in the range of $0.1 \leq C_s \leq 0.3$. Lilly (1962) later extended the Smagorinsky model to turbulence in unstably stratified convection. Due to the stratification an additional parameter, the Richardson number, appears in the expression for the eddy viscosity. The idea that led to Lilly's eddy viscosity is very similar to the above argument underlying the Smagorinsky model: buoyancy production or consumption must also be accounted for in the subgrid energy balance. Thus in the stratified case, the dissipation consists of contribution from both eddy dissipation and thermal diffusion. The Smagorinsky-Lilly eddy viscosity is simply the modified Smagorinsky model with the inclusion of stratification effect

$$\nu_T = (C_s l)^2 \sqrt{2 e_{ij} e_{ij}} \left[1 - \frac{\kappa_T}{\nu_T} Ri_f \right]^{0.5}. \tag{3.3}$$

Here κ_T is the eddy thermal diffusivity, and the flux Richardson number is defined as

$$Ri_f \equiv \frac{g}{2 e_{ij} e_{ij}} \frac{\partial \ln \theta}{\partial r}. \tag{3.4}$$

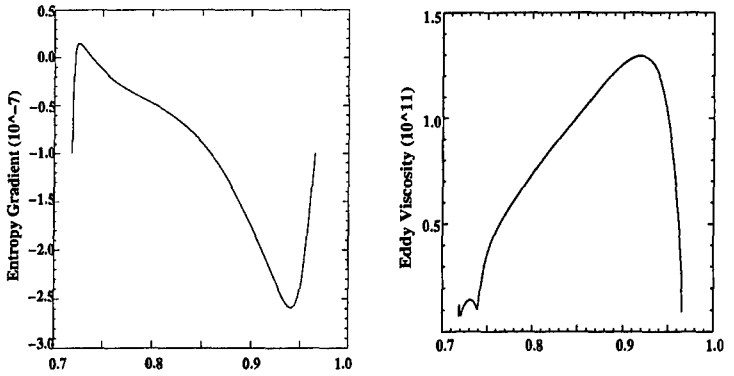

FIGURE 3. The left pannel is the reference entropy gradient (erg/g K m) and the right pannel is the averaged Smagorinsky-Lilly viscosity (cm^2/sec) as functions of r in units of solar radius.

Alternatively, the flux Richardson number can also be defined through entropy as

$$Ri_f \equiv \frac{g}{2e_{ij}e_{ij}} \frac{\partial s_0/\partial r}{C_p}, \tag{3.5}$$

where $\partial s_0/\partial r$ is the reference entropy gradient. In spherical geometry, we choose the length scale l as

$$l \equiv \left(\frac{\Delta(r) r^2}{L_{max}(L_{max}+1)} \right)^{1/3}, \tag{3.6}$$

where $\Delta(r)$ is the radial grid spacing at location r, L_{max} is the maximum (latitudinal) angular mode index.

Figure 3 shows the reference entropy gradient and the averaged Smagorinsky-Lilly viscosity as a function of radius. Near the bottom of the convection zone, the reference entropy gradient is positive, implying a stably stratified region. This corresponds to the small bump seen in the Smagorinsky-Lilly viscosity profile.

In the simulations we start from a stationary configuration with a negative reference entropy gradient throughout the convection zone. The boundary conditions for the velocity are stress free, which are not necessarily realistic but numerically convenient. As we are mostly interested in the differential rotation profile in the convection zone, the parameters and initial reference state are chosen to be the same as the AB case in Brun & Toomre (2002). We first obtain a turbulent convection zone using the mixing length viscosity and thermal diffusivity. As the simulation progresses, the differential rotation profile reaches a statistically stationary state. We then replace the mixing length viscosity and thermal diffusivity with the Smagorinsky-Lilly model with some prescribed constant coefficient C_s. At present we average Smagorinsky-Lilly's eddy viscosity over latitudinal and azimuthal angles. Strictly speaking this is inconsistent with the energy balance principle that gives rise to the eddy viscosity. We are now implementing a local, three-dimensional version of the Smagorinsky-Lilly model, which requires a considerably tedious alteration of the ASH code. For the following results, we present ASH simulations using the averaged Smagorinsky-Lilly eddy viscosity as a test study to see how the differential rotation may differ from that obtained with the "mixing length" viscosity and thermal diffusivity.

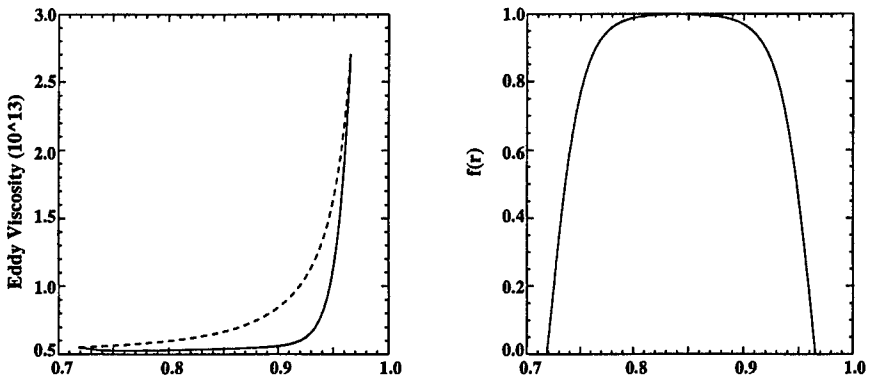

FIGURE 4. Eddy viscosity (cm^2/sec) using the length scale defined in Equation (4.1) (solid line) and the mixing length viscosity (dashed line). On the right is the functional form of $f(r)$ used in constructing the eddy viscosity.

4. Preliminary results and future directions

Our experiences so far show that the averaged Smagorinsky-Lilly eddy viscosity (as shown in figure 3) is too small, and simulations (with resolutions $65 \times 128 \times 256$) blow up soon after the Smagorinsky-Lilly viscosity is activated. A significant difference between the mixing length viscosity and the averaged Smagorinsky-Lilly viscosity is that the eddy viscosity is much smaller at the boundaries. Similar issues arise in large eddy simulations of the atmospheric flows, and it is usually necessary to incorporate a smooth transition from the eddy viscosity to a wall-model viscosity near the boundary. In the solar case, we can combine the mixing length viscosity with the eddy viscosity using a choice of length scale l as follows

$$l^2 = f(r) l_{SL}^2 + (1 - f(r)) l_M^2, \tag{4.1}$$

where l_{SL} is the length scale in Equation (3.6) and l_M is defined as

$$l_M \equiv \frac{1}{C_s} \left(\frac{\nu_M}{\sqrt{2 e_{ij} e_{ij}} \sqrt{1 - Rif}} \right)^{0.5} \tag{4.2}$$

Here $f(r)$ consists of two error functions so that $f(r) = 1$ in the bulk of the convection zone, and $f(r) = 0$ at the boundaries of the convection zone. Figure 4 shows the resultant eddy viscosity (left panel) for a given choice for $f(r)$ (right panel). Figure 5 shows the differential rotation at a instant in time from simulations using the length scale in Equation (4.2).

It is clear from comparing figure 5 and figure 2 that the differential rotation rates are very different near the top of convection zone. In fact the solar observation suggests that the rotation rates decrease near the top of convection zone, which is the opposite of the trend in figure 5. However, near the bottom and in the bulk of the convection zone, the rotation rates from the ASH simulations using the combined eddy viscosity are very similar to those in figure 2. This implies that we may expect to find similar differential rotation profile once we implement a better model than Equation (4.2) for the eddy viscosity near the top of convection zone. Better results may be obtained as well once we implement the fully local Smagorinsky-Lilly's eddy viscosity.

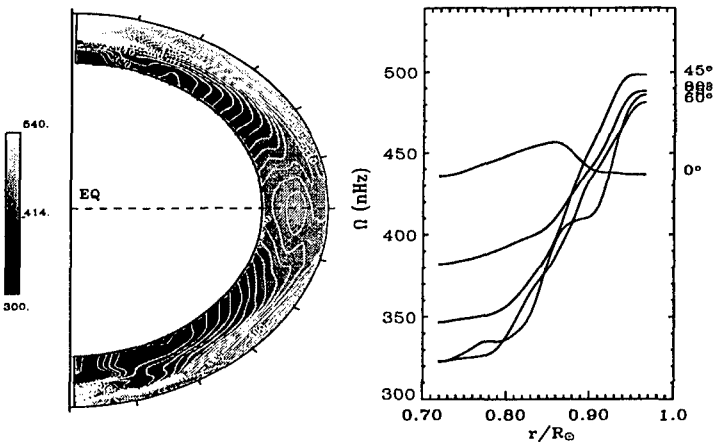

FIGURE 5. Panels (a) and (b): Differential rotation using the eddy viscosity with a transition to the mixing length viscosity near the boundaries of convection zone.

REFERENCES

BRUN, A. S. & TOOMRE, J. 2002 Turbulent convection under the influence of rotation: sustaining a strong differential rotation. *Astrophysical Journal* **570**, 865.

CHRISTENSEN-DALSGAARD, J., PROFFITT, C. R. & THOMPSON, M. J. 1993 Effects of diffusion on solar models and their oscillation frequencies. *Astrophysical Journal* **403**, L75.

CLUNE, T. C., ELLIOTT, J. R., MIESCH, M. S. & TOOMRE, J. 1999 Computational aspects of a code to study rotating turbulent convection in spherical shells. *Parallel Computing* **25**, 361.

GILMAN, P. A. & GLATZMAIER, G. A. 1981 Compressible convection in a rotating spherical shell. I. Anelastic equations. *Astrophysical Journal Suppl.* **45**, 335.

GOUGH, D. O. 1969 The anelastic approximation for thermal convection. *J. Atmo. Sci.* **26**, 448.

LILLY, D. K. 1962 On the numerical simulation of buoyant convection. *Tellus* **24**, 148.

MIESCH, M. S. 1998 Turbulence and convection in stellar and interstellar environments. PhD thesis. University of Coloardo, Boulder.